

## The Energy Spectrum of Fully Developed Turbulence Generated by Random Stirring

M. Lücke and Annette Zippelius  
Physik-Department der Technischen Universität München

Received May 22, 1978

For fully developed turbulence in an incompressible fluid described by the Navier-Stokes equations with Gaussian random forces the relation between the energy spectrum and the stirring mechanism is investigated within a variational approach. Therein, the effect of nonlinear mode coupling is approximated by a wave number dependent eddy viscosity determined via a nonlinear integral equation for the energy spectrum. For various stirring spectra analytic approximations are compared with the solution obtained numerically with a cutoff in the integral kernel which ensures in eddy relaxing processes that the stirring forces exert strain only on scales larger than the eddy size. The results are compared with renormalization group calculations and closure approximations. Random forces injecting energy at a rate  $k^{-1}$  into the wave number band  $dk$  around  $k$  lead to a Kolmogorov distribution of energy. The spectrum of small-scale velocity fluctuations is shown to be universal in the sense that it remains unchanged under variations of the long wavelength stirring spectra.

### 1. Introduction

Statistical theories for fully developed homogeneous turbulence in incompressible fluids investigate either the free decay of an initially prescribed velocity field or the statistically stationary flow generated by random stirring. The stirring forces are thought to inject enough energy into the fluid to balance dissipation caused by viscous energy transfer into molecular degrees of freedom. Whereas the former approach seems to be the more conventional one with closer relation to experimental flow realizability [1], interest in the latter method has been growing over the past few years. A problem continues to be the relation between velocity fluctuations and random forces stirring the fluid.

Renormalization group procedures have been applied [2–4] to study the long wavelength fluctuations in a fluid agitated by random forces whose energy injection rate is powerlaw distributed over wave numbers. A crossover dimension, or equivalently a crossover exponent of the forcing spectrum, was found separating two regimes of weakly and strongly coupled long wavelength velocity fluctuations. Similar re-

sults were obtained by a variational approximation [5], the closure approximation EDQNM [6], and phenomenological arguments [6, 7] similar to those used by Kolmogorov [8].

Fournier and Frisch also investigated stationary scaling solutions of the EDQNM at large wave numbers with an overall power-law forcing. The result [6, 5] shows that the exponent of the energy spectrum depends linearly on the forcing exponent so that a stirring mechanism which injects energy into the wave number band  $dk$  around  $k$  with a power-law rate different from  $k^{-1}$  does not lead to the Kolmogorov  $k^{-5/3}$  energy spectrum. In the case of random forces whose injection rates are not overall power-law distributed one expects, on the other hand, the large wave number inertial range energy spectrum to be independent of long wavelength stirring details. For freely decaying turbulence it has long been suggested [8, 9] that the small-scale behaviour is universal in the sense that small-scale velocity fluctuations superimposed on large-scale eddies are statistically independent of the latter. In such a case

where only local interactions between velocity Fourier modes are relevant, the famous Kolmogorov  $k^{-5/3}$  distribution of energy over wave numbers [8] is obtained by dimensional analysis [8, 10].

In this paper we investigate the relation between forcing and velocity fluctuations in more detail. Section 2 contains the theoretical framework within which the energy spectrum  $E(k)$  of forced turbulence is discussed. Besides basic formulas we present a nonlinear integral equation for  $E(k)$  derived previously [5] within a variational approximation to the generating functional of velocity correlation functions in a stirred fluid. We will introduce into the integral kernel a physically motivated cut-off for nonlinear interactions of Fourier modes which ensures in eddy relaxing processes the random forces to exert strain only on scales larger than the eddy size.

In Section 3 we present the numerical results obtained for various energy injection mechanisms. Consequences of changing the stirring at long wavelengths, intermediate ones and at small scales on the energy spectrum  $E(k)$  are discussed in detail. In an appendix we investigate the behaviour of velocity fluctuations under a uniform convection.

## 2. Theoretical Framework

Consider the Navier-Stokes equation (NSE) for the field  $\mathbf{u}(\mathbf{k}, t)$  of velocity fluctuations in a three-dimensional incompressible fluid stirred by random forces  $\mathbf{f}(\mathbf{k}, t)$

$$(\partial_t + \nu k^2) u_\alpha(\mathbf{k}, t) + i P_{\alpha\beta}(\mathbf{k}) k_\gamma \int \frac{d\mathbf{q}}{(2\pi)^3} u_\beta(\mathbf{q}, t) u_\gamma(\mathbf{k}-\mathbf{q}, t) = f_\alpha(\mathbf{k}, t). \quad (2.1)$$

Here  $\nu$  is the viscosity and  $P_{\alpha\beta}(\mathbf{k})$  denotes the transverse projector

$$P_{\alpha\beta}(\mathbf{k}) = \delta_{\alpha\beta} - \frac{k_\alpha k_\beta}{k^2}. \quad (2.2)$$

It appears when the pressure term is eliminated using the incompressibility condition [10]. The externally imposed random forces  $f_\alpha(\mathbf{k}, t)$  are Gaussian correlated with zero mean and white frequency spectrum

$$\langle \mathbf{f}(\mathbf{k}, t) \cdot \mathbf{f}(\mathbf{k}', t') \rangle = 2(2\pi)^3 \delta(\mathbf{k} + \mathbf{k}') \delta(t - t') D(k). \quad (2.3)$$

The factor 2 is implied by the solenoidal character of the stirring forces. They drive the stochastic process (2.1) and maintain a statistically stationary state balancing the action of the viscous term by injecting energy into the fluid. Viscosity simulates energy dissipation

into molecular degrees of freedom, thus leading to decay of the Fourier amplitudes  $u_\alpha(\mathbf{k}, t)$  at a rate  $\nu k^2$ . The nonlinear mode coupling term transfers energy between the triad of wave numbers  $\mathbf{k}$ ,  $\mathbf{q}$ , and  $\mathbf{k} - \mathbf{q}$ . The rate at which energy is injected into the phase space volume  $d^3 k$  around  $\mathbf{k}$  is measured by  $D(k) d^3 k$ . It is convenient to introduce also  $F(k)$  by

$$F(k) = \frac{k^2}{2\pi^2} D(k) \quad (2.4)$$

such that  $F(k) dk$  is a measure of the input rate into the wave number band  $dk$  around  $k$ .

A principal object of interest of statistical theories of stationary, homogeneous turbulence is the correlation function of velocity fluctuations

$$C(k, \omega) = \frac{1}{2} \int d\mathbf{r} \int dt e^{-i(\mathbf{k} \cdot \mathbf{r} - \omega t)} \langle \mathbf{u}(\mathbf{r}, t) \cdot \mathbf{u}(0, 0) \rangle. \quad (2.5)$$

The energy spectrum  $E(k)$  is related to the equal-time correlation function  $C(k) = C(k, t=0)$  by

$$E(k) = \frac{k^2}{2\pi^2} C(k). \quad (2.6a)$$

$E(k)$  is the spectral distribution of kinetic energy per unit mass over wave numbers such that

$$\int_0^\infty dk E(k) = \frac{1}{2} \langle \mathbf{u}^2 \rangle. \quad (2.6b)$$

A variational principle applied to the generating functional of correlation functions led to a mean field type of approximation [5] for  $C(k, \omega)$  yielding a relaxation dynamics

$$C(k, \omega) = C(k) \frac{2\Omega(k)}{\omega^2 + \Omega^2(k)}. \quad (2.7)$$

The effect of the nonlinear mode-coupling term is approximated here by an eddy viscosity  $\mu(k)$  providing an additional relaxation rate  $k^2 \mu(k)$  to the viscous damping

$$\Omega(k) = k^2 [\nu^2 + \mu^2(k)]^{1/2}. \quad (2.8)$$

Eddy viscosity and energy spectrum  $E(k)$  are coupled via a nonlinear integral equation

$$E(k) = \frac{F(k)}{2\Omega(k)} \quad (2.9)$$

$$\mu^2(k) = \iint_A \frac{dq d\kappa}{k^2} \left(\frac{\kappa}{k}\right)^5 g(k, q, \kappa) \frac{E(q)}{q} \frac{F(k)}{F(\kappa)}. \quad (2.10)$$

The dimensionless kinematical coefficient

$$g(k, q, \kappa) = \frac{1}{2} - \tau_2^2 \tau_3^2 - \frac{1}{2} \tau_1 \tau_2 \tau_3 \quad (2.11)$$

is determined by the three cosines

$$\begin{aligned}\tau_1 &= \frac{q^2 + k^2 - \kappa^2}{2kq}; & \tau_2 &= \frac{\kappa^2 + q^2 - k^2}{2q\kappa}; \\ \tau_3 &= \frac{\kappa^2 + k^2 - q^2}{2k\kappa}\end{aligned}\quad (2.12)$$

of the angles which span a triangle of sidelength  $k, q, \kappa$ . The function  $g(k, q, \kappa)$  is positive, bounded, and unsymmetric under  $\kappa \leftrightarrow q$ . Its relation to the kinematical coefficient  $a$  appearing in closure approximations [7, 10] is  $g(k, q, \kappa) = a_{\kappa q k}$ . The integration range  $\Lambda$  is restricted by momentum conservation to the wave number strip  $|k - q| \leq \kappa \leq k + q$  in the  $q, \kappa$  plane. This reflects the restriction upon the interaction of wave number triads in the nonlinear term of the NSE (2.1).

Within the variational approximation the energy injected by the stirring forces is balanced by the effective damping produced by kinematic and eddy viscosity. The latter shows an UV divergence from contributions  $\kappa \gg k$  (i.e. also  $q \gg k$ ) if  $E(k)$  and  $F(k)$  display reasonable power-law behaviour all the way to infinity. These divergent contributions to the damping of an eddy of size  $k^{-1}$  stem from unphysical processes where the random force stirs the fluid on a scale  $\kappa^{-1}$  being much smaller than the eddy size and thus causes energy transfer from wave vector  $k$  to a much smaller eddy of size  $q^{-1}$ . To prevent such a relaxation mechanism we follow the commonly adopted recipe of closure approximations [6, 7, 10]. There, eddy viscosities entering the triad relaxation time are defined in such a way as to reflect the strain on an eddy of size  $k^{-1}$  exerted only by motions of wave numbers less than  $k$ . In close analogy we introduce a  $\kappa$  cutoff into the integral (2.10) which guarantees the turbulent driving mechanism  $F(\kappa)$  to exert strain on an eddy of size  $k^{-1}$  only via random forces stirring the fluid on scales  $\kappa^{-1}$  larger than  $k^{-1}$ . This seems to be the most direct way to compensate the drawback of the unrestricted variational solution into which enters the bare stirring spectrum and not a renormalized one as one might expect. Note that such a  $\kappa$  cutoff

$$\kappa \leq \alpha k; \quad 0 < \alpha < 1 \quad (2.13)$$

enforces partial locality of the interaction of the wave number triad  $k, q, \kappa$  since momentum conservation implies  $(1 - \alpha)k \leq q \leq (1 + \alpha)k$ . The effect of other, locality-enforcing restrictions will be investigated in the next section.

The parameter  $\alpha$  in (2.13) is chosen such that the wave number  $k_v$ , where viscous dissipation becomes as important as eddy relaxation ( $\mu(k_v) = \nu$ ), is of the order of the dissipative cutoff  $k_d$ . For the latter we

used the Kolmogorov dissipation wave number [10]

$$k_d = \left( \frac{\varepsilon}{\nu^3} \right)^{1/4}. \quad (2.14)$$

The dissipation  $\varepsilon$  is defined by

$$\varepsilon = 2\nu \{k^2\} \quad (2.15)$$

where  $\{k^n\}$  abbreviates the  $n$ 'th moment of the energy spectrum

$$\{k^n\} = \int_0^{k_d} dk k^n E(k). \quad (2.16)$$

Using this notation, one finds the following expressions for the longitudinal integral scale [10]

$$L_p = \frac{3\pi}{4} \frac{\{k^{-1}\}}{\{k^0\}} \quad (2.17)$$

and for the associated Reynolds number [10]

$$R_{L_p} = \frac{\langle \mathbf{u}^2 \rangle L_p}{\nu} = \frac{1}{\nu} \frac{\sqrt{6}\pi}{4} \frac{\{k^{-1}\}}{\{k^0\}^{1/2}} \quad (2.18)$$

or

$$R_{L_p} = \frac{\sqrt{3}\pi}{4} k_d^2 \frac{\{k^{-1}\}}{\{k^0\}^{1/2} \{k^2\}^{1/2}}. \quad (2.19)$$

To obtain (2.19) we replaced in (2.18) the viscosity  $\nu$  by

$$\nu = \sqrt{2} \frac{\{k^2\}^{1/2}}{k_d^2} \quad (2.20)$$

using (2.15) and (2.14). One thus has the choice of expressing  $\nu$  via (2.18) in terms of the Reynolds number or via (2.20) in terms of  $k_d$ . Numerically it is more convenient to solve the integral equation (2.8–2.10) for fixed dissipative cutoff  $k_d$  and determine the Reynolds number  $R_{L_p}$  associated with the solution according to (2.19). With this procedure the physical label  $R_{L_p}$ , which distinguishes solutions of (2.8–2.10) for different forcing spectra  $F(k)$ , is most easily accessible.

### 3. Results

From now on all quantities are understood to be dimensionless, measured in units of a wave number  $K_0$  and an injection rate  $F_0$  characteristic for the externally imposed stirring forces. The energy spectrum, for example, is measured in units of  $F_0^{2/3}/K_0$ , the viscosities  $\nu$  and  $\mu(k)$  are reduced by  $F_0^{2/3}/K_0^2$ , and

the dissipation  $\varepsilon$  has the dimension of  $F_0 K_0$ . Note that (2.8–2.10, 2.20) determine the energy spectrum up to the scale factor  $F_0^{2/3}/K_0$ .

We investigated, for several values of the parameters, two types of stirring spectra: a continuous one

$$F_I(k) = \begin{cases} f_0 k^{y_0} & \text{for } k \leq 0.1 \\ a e^{-a(k-0.2)^2} & \text{for } 0.1 \leq k \leq 1 \\ f_\infty k^{y_\infty} & \text{for } 1 \leq k \end{cases} \quad (3.1)$$

with

$$f_0 = (0.1)^{-y_0} a e^{-a/100}, \quad f_\infty = a e^{-0.64a}$$

and a discontinuous one

$$F_{II}(k) = \begin{cases} f_0 k^{y_0} & \text{for } k \leq 1 \\ f_\infty k^{y_\infty} & \text{for } 1 < k. \end{cases} \quad (3.2)$$

Common to all cases was that more than 96% of the total energy was injected into long wavelength excitations  $k \leq 1$ .

#### a) Technical Details

The solution for the integral Equation (2.8–2.10, 2.20) was obtained by straight-forward iteration starting in every case from the same zeroth approximation and keeping  $k_d = 10^4$  fixed. It took eight to ten iterations to get  $E(k)$  pointwise stable within less than 10% on a logarithmic scale. The convergence behaviour is demonstrated in Figure 1 where  $R_{L_p}$  is plotted as a function of iteration for the representative stirring spectrum shown in Figure 2. The spectral moments  $\{k^n\}$  behave similarly. As another convergence test we used the behaviour of the root mean square deviation

$$[\int d(\ln k) (\ln E_{(n)}(k)/E_{(n-1)}(k))^2]^{1/2}$$

between successive iterations as a function of  $n$ .

In Figure 2 we show the influence of the cutoff procedures for triad interactions in (2.10) on the energy spectrum. Energy was injected into the fluid by a type I stirring mechanism (3.1). The parameters  $y_0 = 4$ ,  $y_\infty = -1$ ,  $a = 10$  imply that in each case 96% of the total energy input rate 4.1 was injected into wave numbers  $k \leq 1$ . For all three cutoffs: (1)  $\kappa \leq 0.9 k$ , (2)  $\kappa \leq 0.5 k$ , and (3)  $\min(k, q, \kappa)/\max(k, q, \kappa) \geq 0.5$   $E(k)$  shows a  $k^{5/3}$  power-law increase for small  $k < 10^{-1}$ , a maximum around 0.2, and a  $k^{-5/3}$  fall-off for large  $k$ . Since these results are characteristic for the stirring spectra (3.1, 3.2) investigated in this work we give, in the following, a more detailed discussion.

#### b) The Spectrum of Long Wavelength Velocity Fluctuations

For the wave numbers down to  $10^{-2}$  as shown in Figure 2, the strong coupling limit holds. There, eddy

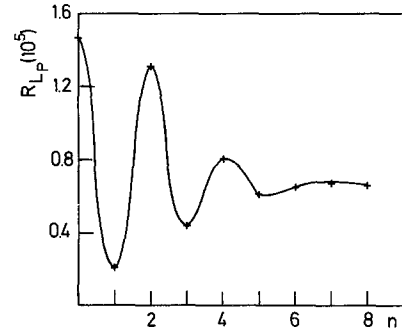


Fig. 1. Reynolds number  $R_{L_p}$  as a function of iteration  $n$  for a representative stirring spectrum. The line is a guide to the eye

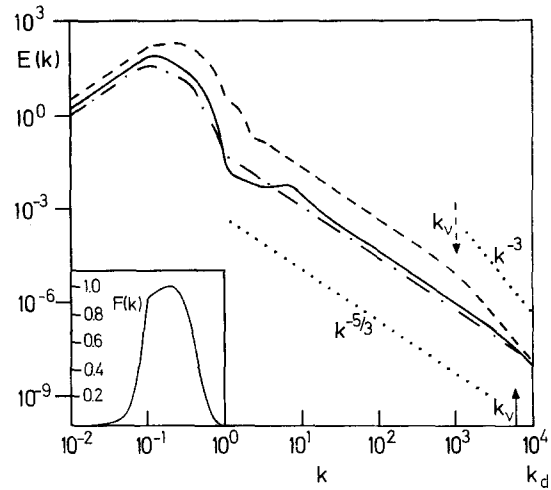


Fig. 2. Influence of cutoff procedures for triad interactions in the eddy viscosity on the energy spectrum of velocity fluctuations. Full curve: cutoff (1)  $\kappa \leq 0.9 k$ ; dashed curve: cutoff (2)  $\kappa \leq 0.5 k$ ; dashed dotted curve: cutoff (3)  $\min(k, q, \kappa)/\max(k, q, \kappa) \geq 0.5$ . Arrows indicate the wave numbers  $k_v$  where eddy relaxation and viscous dissipation are of equal size. The Reynolds numbers are  $R_{L_p}^{(1)} = 6.6 \cdot 10^4$ ,  $R_{L_p}^{(2)} = 2.3 \cdot 10^5$  and  $R_{L_p}^{(3)} = 9.6 \cdot 10^4$ . Insert shows the stirring spectrum  $F(k)$  (3.1) used to obtain the plotted energy spectra

relaxation due to nonlinear mode coupling exceeds viscous damping:  $\mu(k) \gg \nu$ . Then

$$E(k) \simeq \frac{F(k)}{2k^2 \mu(k)} \quad (3.3)$$

shows, for  $k \ll 1$ , power-law behaviour

$$E(k) \simeq e_0 k^{x_0} \quad (3.4)$$

if  $F(k)$  varies like  $f_0 k^{y_0}$ . This can be readily understood by observing that the eddy viscosity reads for a power-law energy spectrum (3.4)

$$\mu^2(k) \simeq e_0 k^{x_0-1} A_0^{(i)}(x_0, y_0) \quad (3.5)$$

where, according to (2.10),

$$A_0^{(i)}(x_0, y_0) = \iint_{\Delta^{(i)}} d\eta d\zeta g(\eta, \zeta) \eta^{x_0-1} \zeta^{5-y_0}. \quad (3.6)$$

The integration range  $\Delta^{(i)}$  is determined by momentum conservation and the cutoffs  $(i)=(1), (2)$  or  $(3)$ . It covers, for  $k \ll 1$ , only values of the reduced variables  $\eta = q/k$  and  $\zeta = \kappa/k$  less than one.

Inserting (3.4) and (3.5) into (3.3) one finds the following power-law solution for the spectrum

$$E(k) \simeq \left[ \frac{f_0^2}{4A_0^{(i)}(x_0, y_0)} \right]^{1/3} k^{\frac{2}{3}y_0-1}; \quad x_0 = \frac{2}{3}y_0 - 1. \quad (3.7)$$

Hence  $E(k)$  displays for small  $k$  a  $k^{5/3}$  behavior if  $y_0 = 4$  as in our case (c.f. Fig. 2). The amplitudes are, on a logarithmic scale, of roughly the same size since the integration ranges  $\Delta^{(i)}$  do not differ drastically. The amplitude is larger in case (2)  $\alpha = 0.5$  than in case (1)  $\alpha = 0.9$  due to the smaller integration range  $\Delta$  entering into  $A_0$ , i.e.  $\mu(k)$ .

In the limit  $k \rightarrow 0$  there will eventually be a crossover  $2\{k^2\}/k_d^4 = \nu^2 \approx \mu^2(k) \sim k^{x_0-1}$  to the weak coupling limit [5] whenever  $x_0$  is larger than one, i.e. for  $y_0 > 3$ . However, the crossover happens because of the small dissipation length  $k_d^{-1}$ , well below the smallest wave number  $10^{-2}$  shown in Figure 2. Hence, the small  $k$  energy spectra of Figure 2 still display strong coupling behaviour despite the forcing exponent  $y_0 = 4$ . Only in the limit of very small  $k$  where  $\nu \gg \mu(k \rightarrow 0)$  one enters the weak coupling regime characterized according to (2.8, 2.9) by  $x_0 = y_0 - 2$ . And using relation (3.5)  $\mu^2(k) \sim k^{x_0-1}$  one recovers for  $k \rightarrow 0$  the crossover exponent  $x_0 = 1$ , i.e.  $y_0 = 3$  also from the weak coupling side. The relations  $x_0 = \frac{2}{3}y_0 - 1$  (3.7) for  $y_0 < 3$  and  $x_0 = y_0 - 2$  for  $y_0 > 3$  between exponents of the energy spectrum and the stirring spectrum in the limit  $k \rightarrow 0$  have been derived with renormalization group techniques by Fournier [4].

### c) Energy-Containing Range at Intermediate $k$

The maximum in  $E(k)$  around 0.2 and the subsequent steep decrease reflect the energy injection distribution  $F(k)$  (3.1) showing a peak at  $k = 0.2$ . The longitudinal integral scale  $L_p$  varies with cutoff between 0.44 and 0.55. Hence, in the stationary state, most of the energy is contained in the large-scale eddies into which most of the energy has been injected.

The dip in the energy spectrum for wave numbers roughly between 1 and 6 in the cutoff case (1)  $\alpha = 0.9$  is due to an enhancement of the eddy viscosity  $\mu(k)$ : For values of  $k$  between  $\alpha^{-1}$  and  $(1-\alpha)^{-1}$  (in our case for  $1.1 < k < 10$ ) the integration range  $\Delta^{(1)}$  allows triad interactions of wave numbers  $\kappa > 1$  with wave numbers  $q < 1$  which correspond to the energy-containing range of  $E(q)$ . For these combinations the integrand in (2.10) is large.

The energy spectrum displays a small bump around  $k \simeq 7.4$  as a consequence of the dip: The integration range  $\Delta^{(1)}$  extends, for that  $k$  value, over wave numbers  $q$  for which  $E(q)$  shows the dip. This yields a relative decrease of  $\mu(k)$ . The other two cutoff procedures enforce a more local triad interaction. Hence  $E(k)$  shows less structure for wave numbers  $1 < k < 10$  and the inertial range begins already at smaller values of  $k$ .

### d) The Inertial Range Spectrum

For all three cases there is an inertial range with a  $k^{-5/3}$  decrease. It can be understood with an argumentation completely analogous to the one presented for the explanation of the small  $k$  behaviour (c.f. discussion connected with (3.3–3.7)). One finds in the strong coupling limit a power law  $E(k) \sim k^{x_\infty}$

$$E(k) \simeq \left[ \frac{f_\infty^2}{4A_0^{(i)}(x_\infty, y_\infty)} \right]^{1/3} k^{x_\infty}; \quad x_\infty = \frac{2}{3}y_\infty - 1 \quad (3.8)$$

for a power law forcing  $F(k) = f_\infty k^{y_\infty}$  in agreement with results of the EDQNM [6]. Here  $A_\infty^{(i)}(x_\infty, y_\infty)$  is determined in direct analogy to (3.6) since for  $k \gg 1$  contributions to  $A_\infty^{(i)}$  from  $\kappa < 1$  are negligible (see below). Equation (3.8) explains the appearance of the Kolmogorov spectrum  $k^{-5/3}$  in Figure 2 as a result of a power law forcing  $k^{-1}$  for large  $k$ . The Kolmogorov constant  $C_K$  derived from the inertial range parametrization  $E(k) = C_K \varepsilon^{2/3} k^{-5/3}$  has the value (1)  $C_K = 0.93$ , (2)  $C_K = 3.2$ , and (3)  $C_K = 0.7$  respectively for the three cases shown in Figure 2.

Note that the locality of triad interactions entered decisively into the derivation of (3.8): All three integration ranges  $\Delta^{(i)}$  are local in  $q$  covering only wave numbers  $q$  of the order of  $k$ . Whereas  $\Delta^{(3)}$  is also local in  $\kappa$ ,  $\Delta^{(1)}$  and  $\Delta^{(2)}$  allow triad interactions with wave numbers  $\kappa \ll k$ . For these wave numbers  $F(k)/F(\kappa) \ll 1$  so that their contribution to  $\mu(k)$  is negligible. Hence local interactions dominate the eddy relaxation.

The effective locality of the triad interactions entails the existence of an inertial range: There the form of the energy spectrum  $E(k)$  (3.8) does neither depend on the details of the energy injection mechanism at long wavelengths or on details of the energy containing eddies of size  $L_p$  nor on the form of the viscous energy drainage simulated here by the cutoff at  $k_d$ . It does, however, depend on the forcing at large wave numbers. A different power-law forcing at large  $k$  yields according to (3.8) another power law for  $E(k)$  [6].

### e) Viscous Energy Dissipation

Equation (3.8) was derived for  $\mu(k) \gg \nu$ . Viscous dissipation equals eddy relaxation at the wave number

$$k_v \simeq \left[ \frac{k_d^4 e_\infty A_\infty^{(i)}}{2\{k^2\}} \right]^{\frac{1}{1-x_\infty}} \quad (3.9)$$

where we used the strong coupling expression

$$\mu^2(k) \simeq e_\infty k^{x_\infty-1} A_\infty^{(i)}(x_\infty, y_\infty)$$

with  $e_\infty$  denoting the prefactor in (3.8). For the ensuing explanatory discussion it is sufficient to approximate  $\{k^2\}$  by  $e_\infty k_d^{x_\infty+3}$  since the dominant contribution to the second moment comes from large  $k$  and since  $k_v$  is of the order of  $k_d$ . Inserting this estimate of  $\{k^2\}$  into (3.9) one finds that

$$k_v \simeq k_d [A_\infty^{(i)}]^{-\frac{1}{1-x_\infty}} \quad (3.10)$$

does not depend on  $e_\infty$  nor on  $f_\infty$ . This has been verified by varying  $f_\infty$  and with it  $e_\infty$ . In accordance with (3.10) we have found numerically that the only effect of increasing  $k_d$  was to enlarge the inertial range and to yield a larger Reynolds number (2.19). The qualitative formula (3.10) also explains why  $k_v$  for cutoff (1) (full arrow in Fig. 2) is larger than for cutoff (2) (dashed arrow):  $A_\infty^{(1)}$  is larger than  $A_\infty^{(2)}$  since the integration range  $\Delta$  in (2.10) is larger for  $\alpha=0.9$ . For cutoff (3) we found  $\mu(k) > \nu$  for all wave numbers shown in Figure 2. Since cutoff (2), on the other hand, gave a value of  $k_v$  too small compared with  $k_d$ , we will from now on consider only cutoff procedure (1). Then the wave vector  $k_v$  where  $\mu(k_v) = \nu$  is located just below the dissipative cutoff  $k_d$ . Beyond  $k_v$  the viscous dissipation range  $\nu \gg \mu(k)$  begins where  $E(k)$  has the form

$$E(k) \simeq \frac{F(k)}{2\nu k^2} \sim k^{y_\infty-2}. \quad (3.11)$$

For a stirring spectrum with  $y_\infty = -1$   $E(k)$  displays a final  $k^{-3}$  fall-off to be seen in Figure 2.

*f) Variation of the Energy Injection at Large k*

In Figure 3 we show the results of decreasing the stirring strength of a type I injection spectrum (3.1) at large  $k$ . In all three cases shown  $y_0=4, y_\infty=-1$ . The injection rate  $f_\infty$  was varied from  $9.6 \times 10^{-3}$  to  $5.5 \times 10^{-5}$  by a factor of about 175 and the percentage of injection into large wave-number eddies by a factor of about 250 (due to the form of (3.1) the total energy input increased from 4.3 to 6.2 upon increasing  $a$  from 11 to 20).

There was no significant change of the energy spectrum at large  $k$ . The only form change occurred at the dip becoming more pronounced. The Reynolds number dropped from  $R_{L_p} = 5.9 \times 10^4$  to  $2.3 \times 10^4$  mostly since the longitudinal integral scale decreased from  $L_p = 0.41$  to  $L_p = 0.21$ . That can be traced back to the

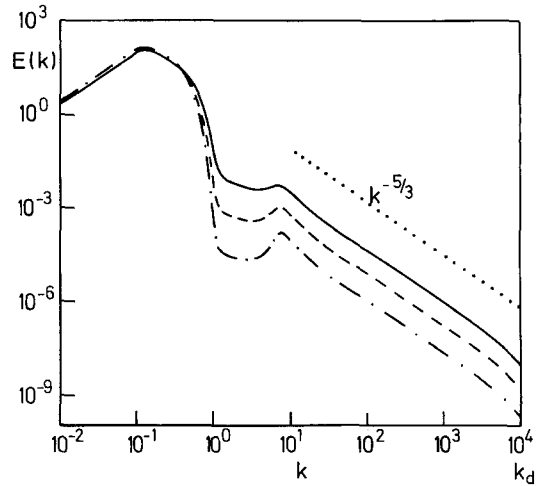


**Fig. 3.** Energy spectrum resulting from a type I stirring (3.1) with  $y_0=4, y_\infty=-1$  for various large wave number injection amplitudes  $f_\infty = a e^{-0.64a}$ . Full curve:  $a=11$  (2% of total input at  $k>1$ ); dashed curve:  $a=15$  (0.18% of total input at  $k>1$ ); dashed dotted curve:  $a=20$  (0.008% of total input at  $k>1$ )

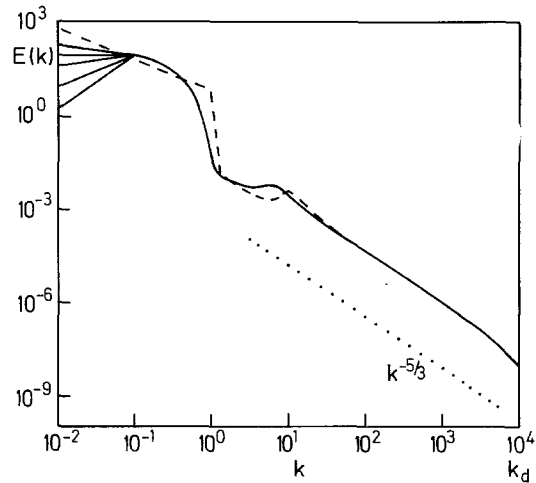


**Fig. 4.** Energy spectra for various type I stirring mechanisms (full curves) and for a representative type II injection (dashed curve) with a constant energy input up to  $k=1$ . The long wavelength exponents  $y_0$  for the type I stirring spectra were (from top to bottom) 1, 1.5, 2, 3, 4

injection spectrum (3.1) becoming sharper peaked around  $k=0.2$  with decreasing  $f_\infty$  (increasing  $a$ ). The Kolmogorov constant for the three curves in Figure 3 remained unchanged  $C_K=0.9$ . Note that  $k_v$  is not affected by varying  $f_\infty$  or the size of  $E(k)$ , as discussed earlier.

*g) Variation of the Long Wavelength Stirring Spectrum*

In Figure 4 we show the effect of varying the injection mechanism at long wavelengths  $k \leq 1$ , keeping

its small-scale characteristics  $y_\infty = -1$ ,  $f_\infty = 10 e^{-6.4}$  fixed. The Reynolds numbers are  $R_{L_p} = 4.3 \times 10^4$  for the dashed curve and  $R_{L_p} = 6.5 \times 10^4$  for all full curves. We also investigated a stirring spectrum with  $F(k=0) \neq 0$  of the form  $F(k) = f_0 - a(k - k_0)^2$  for  $k \leq 1$ . Here  $k_0$  was varied between 0.1 and 0.3 and  $f_0$  was fixed by requiring  $F(k)$  to be continuous at  $k=1$ . The resulting energy spectrum shows only minor modifications compared to the  $k^0$  stirring of type II: The discontinuity at  $k=1$  gets rounded while deviations at very small wave numbers and in the inertial range are within pencil's width.

Obviously, the large  $k$  inertial range is universal in the sense that different long wavelength (power law) stirring spectra do not modify velocity correlations over small scales. This is in a sense a trivial consequence of the locality of triad interactions. A less trivial consequence of the variational approximation (2.8–2.13) is that it predicts the same inertial range power law (3.8) as the EDQNM [6] and the same long wavelength behaviour of velocity fluctuations as renormalization group procedures [4, 2]. The long wavelength energy spectrum displays according to (3.7) in the strong coupling regime exponents  $x_0 = \frac{2}{3}y_0 - 1$  to be seen in Figure 4 for various  $y_0$ .

## Appendix

Here we will investigate the behaviour of the variational approximation (2.7–2.13) when a uniform velocity  $\mathbf{v}$  is superimposed on the field of velocity fluctuations  $\mathbf{u}(\mathbf{r}, t)$ . The effect of such a uniform convection on the NSE (2.1) is only a phase change  $\mathbf{u}(\mathbf{k}, t) \rightarrow \mathbf{u}(\mathbf{k}, t) e^{i\mathbf{k} \cdot \mathbf{v}t}$  and  $\mathbf{f}(\mathbf{k}, t) \rightarrow \mathbf{f}(\mathbf{k}, t) e^{i\mathbf{k} \cdot \mathbf{v}t}$ . Or, stated in other words: the NSE (2.1) are invariant under the Galilean transformation  $\mathbf{u}'(\mathbf{r}', t) = \mathbf{u}(\mathbf{r} + \mathbf{v}t, t) + \mathbf{v}$  if also the random forces are Galilean invariant  $\mathbf{f}'(\mathbf{r}', t) = \mathbf{f}(\mathbf{r} + \mathbf{v}t, t)$ . Hence equal-time correlation functions are not affected by a uniform convection.

The linear NSE

$$(\partial_t + \nu k^2) \mathbf{u}(\mathbf{k}, t) = \mathbf{f}(\mathbf{k}, t) \quad (\text{A.1})$$

is not Galilean invariant. It is, however, not changed by the addition of a uniform velocity. Note that showing invariance under uniform convection rather than invariance under Galilean transformations is physically relevant for a statistical theory of turbulence. The variational result [5] is equivalent to the following equation of motion

$$(\partial_t + \Omega(k)) \mathbf{u}(\mathbf{k}, t) = \mathbf{f}(\mathbf{k}, t). \quad (\text{A.2})$$

Here  $\Omega(k)$  is determined by the solution of the integral equation (2.8–2.13) for  $E(k)$ . Like the linear

NSE, Equation (A.2) is not Galilean invariant. It is, however, not changed by adding to  $\mathbf{u}(\mathbf{k}, t)$  a uniform field  $\mathbf{v}(2\pi)^3 \delta(\mathbf{k})$  if the total effective relaxation rate  $\Omega(k)$  vanishes for  $k \rightarrow 0$ .

This is trivially the case for forcing spectra  $F(k)$  with a long wavelength exponent  $y_0 > 3$ . Then the weak coupling limit  $\nu \gg \mu(k \rightarrow 0)$  holds where  $E(k \rightarrow 0) \sim k^{y_0-2}$  (2.8) and  $\mu^2(k \rightarrow 0) \sim k^{y_0-3}$  (3.5) and consequently  $\Omega(k) \simeq \nu k^2$ . The expression  $A_0$  (3.6)

$$A_0^{(1)}(y_0 - 2, y_0) = \int_{1-\alpha}^{1+\alpha} d\eta \eta^{y_0-3} \int_{|1-\eta|}^{\alpha} d\zeta \zeta^{5-y_0} g(\eta, \zeta) \quad (\text{A.3})$$

entering into  $\mu^2(k)$  (3.5) converges for  $y_0 < 7$ . Note the dependence of the results in this appendix on the cutoff procedure (2.13) for the triad interactions.

In the strong coupling limit ( $\mu(k \rightarrow 0) \gg \nu$ ) enforced by long wavelength injection spectra with exponent  $y_0 < 3$  we found in Section 3:  $E(k \rightarrow 0) \sim k^{\frac{2}{3}y_0-1}$  (3.7) and  $\mu^2(k \rightarrow 0) \sim k^{\frac{2}{3}y_0-2}$  (3.5). Then the relaxation rate behaves as  $\Omega(k \rightarrow 0) \sim k^{1+y_0/3}$ . The conclusion to be drawn from this result is that forcing the fluid at long wavelengths by power-law distributed injection rates leads to velocity correlations invariant under uniform convection as long as the exponent  $y_0$  is larger than  $-3$ , i.e. for  $x_0 = \frac{2}{3}y_0 - 1 > -3$ . The lower bound  $x_0 = -3$  for the exponent of the energy spectrum coincides with the lower bound for convergence of the transfer integral in the EDQNM closure approximation [6].

Discussions with J.D. Fournier and U. Frisch are gratefully acknowledged.

## References

1. For an extensive review see Monin, A. and Yaglom, A.M.: Statistical Fluid Mechanics, Vol. 2. Cambridge: MIT Press 1975
2. Forster, D., Nelson, D.R., Stephen, M.J.: Phys. Rev. A **16**, 732 (1977)
3. Lovesey, S.W.: J. Phys. C **10**, 1781 (1977)
4. Fournier, J.D.: Thesis, University of Nice 1977
5. Lücke, M.: Phys. Rev. A July 1978
6. Fournier, J.D., Frisch, U.: Phys. Rev. A **17**, 747 (1978)
7. Rose, H.A., Sulem, P.L.: Journal de Physique **39**, 441 (1978)
8. Kolmogorov, A.N.: C.R. Ac. Sc. URSS **30**, 301 (1941)
9. For a review see ref. 10
10. Orszag, S.A. in: Fluid Dynamics, ed. Balian, R. and Peube, J.L., pp. 235–374. New York: Gordon and Breach 1977

M. Lücke  
Annette Zippelius  
Physik-Department  
der Technischen Universität München  
Theoretische Physik  
D-8046 Garching  
Federal Republic of Germany